Water Resources Research

RESEARCH ARTICLE
10.1029/2024WR037907

Evapotranspiration and Rainfall Effects on Post-Storm Salinization of Coastal Forests: Soil Characteristics as Important Factor for Salt-Intolerant Tree Survival

Giovanna Nordio[1] and **Sergio Fagherazzi**[1]

[1]Department of Earth and Environment, Boston University, Boston, MA, USA

Key Points:

- Evapotranspiration and rainfall affect post-storm surge soil salinity in the root zone of coastal forests
- In clay loam soils, post-storm surge salinity stratification is beneficial for root uptake
- Time to recover to pre-storm soil salinity values depends on evapotranspiration and rainfall ratios and soil properties

Supporting Information:

Supporting Information may be found in the online version of this article.

Correspondence to:

G. Nordio,
nordiog@bu.edu

Citation:

Nordio, G., & Fagherazzi, S. (2024). Evapotranspiration and rainfall effects on post-storm salinization of coastal forests: Soil characteristics as important factor for salt-intolerant tree survival. *Water Resources Research*, *60*, e2024WR037907. https://doi.org/10.1029/2024WR037907

Received 8 MAY 2024
Accepted 7 SEP 2024

Author Contributions:

Conceptualization: Giovanna Nordio, Sergio Fagherazzi
Data curation: Giovanna Nordio
Formal analysis: Giovanna Nordio
Funding acquisition: Sergio Fagherazzi
Investigation: Giovanna Nordio, Sergio Fagherazzi
Methodology: Giovanna Nordio, Sergio Fagherazzi
Project administration: Sergio Fagherazzi
Resources: Sergio Fagherazzi
Supervision: Sergio Fagherazzi
Validation: Giovanna Nordio
Visualization: Giovanna Nordio

Abstract Flooding and salinization triggered by storm surges threaten the survival of coastal forests. After a storm surge event, soil salinity can increase by evapotranspiration or decrease by rainfall dilution. Here we used a 1D hydrological model to study the combined effect of evapotranspiration and rainfall on coastal vegetated areas. Our results shed light on tree root uptake and salinity infiltration feedback as a function of soil characteristics. As evaporation increases from 0 to 2.5 mm/day, soil salinity reaches 80 ppt in both sandy and clay loam soils in the first 5 cm of soil depth. Transpiration instead involves the root zone located in the first 40 cm of depth, affecting salinization in a complex way. In sandy loam soils, storm surge events homogeneously salinize the root zone, while in clay loam soils salinization is stratified, partially affecting tree roots. Soil salinity stratification combined with low permeability maintain root uptakes in clay loam soils 4/5-time higher with respect to sandy loam ones. When cumulative rainfall is larger than potential evapotranspiration ET_p (ET_p/Rainfall ratios lower than 1), dilution promotes fast recovery to pre-storm soil salinity conditions, especially in sandy loam soils. Field data collected after two storm surge events support the results obtained. Electrical conductivity (a proxy for salinity) increases when the ratio ET_p/Rainfall is around 1.76, while recovery occurs when the ratio is around 0.92. In future climate change scenarios with higher temperatures and storm-surge frequency, coastal vegetation will be compromised, because of soil salinity values much higher than tolerable thresholds.

1. Introduction

Sea level rise (SLR) and storm surge events are the main drivers of coastal forest retreat (Carr et al., 2020; Doyle et al., 2010; Fagherazzi et al., 2019; Kearney et al., 2019; Kirwan & Gedan, 2019; Schieder and Kirwan, 2019). Low-lying zones, usually topography-controlled, are the most affected by flooding and saltwater intrusion from above (Cantelon et al., 2022). Here surface flooding due to storm surge events is compounded to saturation overland runoff triggered by an increase in groundwater table (Befus et al., 2020; Gleeson et al., 2011; May, 2020; Michael et al., 2013; Rotzoll & Fletcher, 2013). Saltwater intrusion undermines tree seed germination more than mature tree survival (Fernandes et al., 2018; Kearney et al., 2019; Williams et al., 1999).

In coastal forests, 70% of the active roots typically occupy the top 40 cm of soil (Mou et al., 1995; Parker & Lear, 1996; Xu et al., 2016) and vegetation controls the soil-atmosphere exchanges within the unsaturated zone. Flooding events affect the available oxygen content in the soil and decrease the soil redox potential, net carbon accumulation, and stomatal conductance thus slowing the photosynthetic activity of flood intolerant vegetation species (Pezeshki et al., 1999). Salinity intrusion exacerbates the flooding effects (Pezeshki, 1992), causing osmotic and ionic stress in non-salt tolerant vegetation species at different growing stages (Munns & Tester, 2008). During surges, coastal groundwater and soil edaphic conditions become homogenous, reducing hydrological differences across the forest (Nordio, Gedan, & Fagherazzi, 2024; Nordio et al., 2023) and affecting ecological patterns (Allen & Lendemer, 2016; Burkett et al., 2008; Konar et al., 2013).

Storm surge events, occurring on short temporal scales, trigger saltwater intrusion and rapid vertical infiltration. Recovery time to pre-storm conditions are dependent on soil characteristics (Yang et al., 2018). For example, salinization triggered by Hurricane Jeanne in 2004, a category 5 cyclone, lasted up to 8 years in a low-permeability surficial aquifer (Xiao et al., 2019). In 2013, saltwater intrusion due to supertyphoon Haiyan in sandy aquifers of Samar Island, Philippines was felt up to 1–2 years after the event (Cardenas et al., 2015). Time to recovery is likely affected by external factors and ecohydrological feedbacks. Salinity conditions established after the storm surge can be exacerbated by evaporation, with detrimental effects for non-salt tolerant ecosystems.

Writing – original draft: Giovanna Nordio
Writing – review & editing: Giovanna Nordio, Sergio Fagherazzi

In intertidal areas, salinity values are often higher than those recorded in seawater over the post-surge period (Geng & Boufadel, 2015; Geng et al., 2016, 2021; Rajmohan et al., 2021). This often occurs in the upper intertidal zone, where tides and waves seldom dilute pore water salinity (Geng et al., 2016). Groundwater modeling conducted on sandy beaches suggests a doubling in salinity in the intertidal zone when evaporation is considered (Geng & Boufadel, 2015). Rainfall can dilute soil salinity when soil water content is lower than saturation (Sumner & Belaineh, 2005). Geng and Boufadel (2017) showed that moderate rainfall events significantly reduced salinity in the first 10 cm of soil in a sandy beach. A rainfall rate of 1.4 cm/hr decreased soil salinity to zero.

In coastal vegetated areas the effects of plant transpiration compounds to soil evaporation. Previous studies have investigated root-zone salinization induced by plant transpiration in agricultural fields (Aragues et al., 2014; Nachshon, 2018; Rengasamy et al., 2003; Smets et al., 1997; Wang et al., 2023). The major source of solutes in agriculture was found to be the shallow and salt rich groundwater and the salt rich irrigation water (Nachshon, 2018). Few studies have brought attention on these dynamics in coastal forests (e.g., Xiao et al., 2019), where the major sources of saltwater intrusion are storm surges. Here we want to quantify the effects of evapotranspiration and rainfall on soil salinity after storm surge events. To this end, we use a 1D hydrological model (HYDRUS) in the presence of vegetation. HYDRUS 1D has been used to estimate water (e.g., Tan et al., 2015) and salt infiltration (e.g., Yang et al., 2019; Zeng et al., 2014) in agricultural fields during irrigation and to estimate evapotranspiration of in-situ vegetation (e.g., Li et al., 2014). Nordio, Pratt, et al. (2024) proposed using HYDRUS 1D to study salinity distribution in the root zone following storm surge events across various soil types. Saltwater intrusion in coastal groundwater has also been studied using more complete 2D variable saturation and density models (e.g., Cantelon et al., 2022; Geng et al., 2016; Paldor & Michael, 2021; Stanic et al., 2024; Yang et al., 2018). As far as we know, none of these studies considered the ecological response in terms of root uptake and the feedback between transpiration and salt-water intrusion in the soil. In this research, we focus on the dynamics of the root zone, investigating the response of coastal trees to soil salinity values exceeding tolerable thresholds. Our simplified model allows us to: (a) estimate the impact of different evaporation and transpiration rates on post-surge salinity; (b) determine how soil salinity increases due to evapotranspiration in different types of soil; (c) assess the beneficial effect of post-surge rainfalls and (d) estimate the root uptake response at different evaporation and rainfall rates. Finally, the results obtained from the HYDRUS 1D simulations are compared to data collected during in-situ campaigns.

2. Methods

2.1. Model Description

HYDRUS 1D is a one-dimensional model simulating water, heat, and solute movement in a variably saturated medium (Šimůnek et al., 2018). To simulate water flow along the vertical axis, the Richards's Equation 1 is numerically solved using Galerkin finite element method, together with appropriate initial and boundary conditions (Celia et al., 1990).

$$\frac{\partial \theta}{\partial t} = \frac{\partial}{\partial z}\left[K(\theta)\left(\frac{\partial h}{\partial z} + 1\right)\right] - S(z, t) \tag{1}$$

where z is the vertical axis (soil depth), t is the time, θ is the water content (L/L), h is the pressure head (L), $K(\theta)$ is the hydraulic conductivity (L/T) that depends on water content and reaches a maximum value K_s in saturated conditions, and $S(z, t)$ is a sink term usually linked to root uptake (L/T). Van Genucthen Equation 2 was chosen to relate h to θ (van Genuchten, 1980).

$$\theta(h) = \begin{cases} \theta_r + \dfrac{\theta_s - \theta_r}{[1 + |\alpha h|^n]^m} & h < 0 \\ \theta_s & h \geq 0 \end{cases} \tag{2}$$

Where θ_r is the water content at wilting point [L/L], θ_s is the water content at saturation [L/L] and m, n and α are the parameters of the van Genuchten soil curve. $K(\theta)$ in Equation 1 is calculated for each degree of saturation in the soil using Equation 3:

$$K(\theta) = K_s S_e^{1/2}\left[1 - \left(1 - S_e^{\frac{1}{m}}\right)^m\right]^2 \quad (3)$$

Where S_e is the saturation degree, and it is calculated using Equation 4:

$$S_e = \frac{\theta(h) - \theta_r}{\theta_s - \theta_r} \quad (4)$$

To simulate solute movement, the advection-dispersion equation Equation 5 is numerically solved in HYDRUS 1D:

$$\frac{\partial(\theta C)}{\partial t} = \frac{\partial}{\partial z}\left(D\theta\frac{\partial C}{\partial z}\right) - \frac{\partial}{\partial z}(q_w C) \quad (5)$$

where C is the solute concentration in (M/L), q_w is the water flux [L/T] and D is the dispersion coefficient [L/T].

The sink term $S(z, t)$ is linked to the actual root uptake, which is dependent on soil water content and salinity and external climatic conditions. This can be expressed as:

$$S(z, t) = \beta(h)\rho(C)\, r(z)\, T_p \quad (6)$$

where $\beta(h)$ is a dimensionless function of the soil water pressure head and ranges from 0 to 1, $\rho(C)$ is a function of solute concentration, $r(z)$ represents the relative intensity of the potential root water uptake distribution in the root zone as a function of depth, and Tp is the potential vegetation transpiration as a function of climatic variables. Feddes's model is used to describe $\beta(h)$ as follows:

$$\beta(h) = \begin{cases} \dfrac{h - h_4}{h_3 - h_4} & h_3 > h > h_4 \\ 1 & h_2 \geq h \geq h_3 \\ \dfrac{h - h_1}{h_2 - h_1} & h_1 > h > h_2 \end{cases} \quad (7)$$

where h_1 delimits the anoxic phase, h_1 and h_2 the hypoxic phase, h_2 and h_3 delimit a constant rate phase where actual root water uptake equals the potential root uptake, h_3 and h_4 delimit the decrease in root water uptake and h_4 the permanent wilting phase (de Melo & van Lier, 2021). Root water uptake is additionally reduced if the soil salinity is higher than a threshold that limits normal photosynthetic activity in each vegetation species. A threshold model is chosen to consider the salinity effects on root water uptake as multiplicative to water stress. According to Maas (1990), a root water uptake salinity stress response function is expressed as:

$$\rho(C) = 1 - 0.01s(C - c_T) \quad (8)$$

where C is the soil salt concentration, c_T is the value of the minimum osmotic head (the salinity threshold) above which root water uptake occurs without a reduction and s is the slope of the curve determining the fractional decline in root water uptake per unit increase in salinity above the threshold.

HYDRUS 1D simulates constant-density flows. In coastal areas, where salinity intrusion is exacerbated, the use of variable-density model is often preferred, but more so in the saturated zone, where the effect of density can be significant (Younes et al., 2022).

2.2. Model Set-Up

According to Fan et al. (2013), in low-lying coastal areas unsaturated soil depth is between 25 and 250 cm below the ground surface. In our simulations, we chose two soil columns of L = 120 cm consisting of sandy loam or clay loam, with edaphic characteristics derived from the HYDRUS 1D database (Table S1 in Supporting

Table 1
Scenarios of Potential Evaporation and Transpiration After a Storm Surge Event

Scenario	Potential evaporation (mm/day)	Potential transpiration (mm/day)
Scenario 1	1.0	0.5
Scenario 2	1.0	1.0
Scenario 3	1.0	2.0
Scenario 4	2.0	0.5
Scenario 5	2.0	1.0
Scenario 6	2.0	2.0
Scenario 7	0.5	0.5
Scenario 8	0.5	1.0
Scenario 9	0.5	2.0

Information S1). To solve the solute transport Equation 5, bulk density ρ [M/L], and longitudinal dispersivity D_L [L] were respectively set to 1.4 g/cm^3 (Yu et al., 1993) and to 7 cm (Vanderborght & Vereecken, 2007) for all simulations.

We assume that the forest is dominated by *Pinus taeda* (loblolly pines), a common tree along the eastern US shore. This species is moderately flooding and salt tolerant (Pezeshki, 1992). Most of the active roots occupy the first 40 cm of the soil column and we suppose that they equally contribute to the potential water uptake ($r(z) = 1$) in both soil types. This simplification is adopted because data on root distribution in different soils are scarce. Since it was not possible to derive values for h_1, h_2, h_3 and h_4 for *Pinus taeda* from the literature, we used values reported in Rabbel et al. (2018) for *Picea abies* (Norway spruce): $h_1 = 0$ cm, $h_2 = -600$ cm, $h_3 = -1{,}200$ cm, $h_4 = -15{,}000$ cm. For the threshold model c_T and s are respectively fixed at 5 ppt and 2 according to previously published data (Poulter et al., 2008; Woods et al., 2020). The osmotic coefficient was set to 1 as suggested for multiplicative models. We first simulated a storm surge as a prescribed water column on the ground surface. Therefore, the water flow boundary condition was set as "variable pressure" at the ground surface level. For simplicity, we fixed the surge flooding to a constant water depth of 15 cm for a duration of 1 day according to data collected in Fagherazzi and Nordio (2023). At the soil column bottom, we set a Dirichlet boundary condition with $\theta(L, t) = \theta_s$, assuming L as the maximum groundwater table depth from the ground surface. As initial condition we set a water content of 0.25 cm^3/cm^3 along the entire soil column. Similarly, for the salt concentration, we set a Dirichlet boundary condition with constant concentration, equal to the concentration of saline water of the surge at the top boundary (25 ppt) and a Neuman type, with zero concentration gradient at the bottom. We set a salt concentration of 5 ppt along the entire soil column as initial condition. The results from this first simulation at the end of the storm surge are in turn used as initial conditions for the next simulations where we investigate the dynamics of post-surge soil salinity. To this end, for these second set of simulations, we assign atmospheric boundary conditions at the topsoil and ran the model for 100 days (∼one season) with different soil potential evaporation rates, vegetation potential transpiration rates, and rainfall events. Potential evaporation and transpiration rates are maintained equal over the simulated period, considering these values as a mean seasonal value. The model setup for post-storm simulations is summarized in Figure S1 in the Supporting Information S1.

2.3. Scenarios

To study evapotranspiration effects on soil salinity, we ran 38 scenarios in total. These included three types of scenarios: evaporation-only, transpiration-only, and combined evapotranspiration (i.e., both evaporation and transpiration). We chose five potential evaporation rates and five potential transpiration rates for both sandy loam and clay loam soil columns. We first considered evaporation and transpiration separately and then studied the combined effect on the soil and the tree root uptake response. Evaporation-only scenarios are representative of a ghost forest, where canopies are barren. Transpiration-only scenarios are representative of a very dense forest canopy. Potential evaporation (E_p) and transpiration (T_p) rates of 0.5 mm/day, 1 mm/day, 1.5 mm/day, 2 mm/day and 2.5 mm/day were selected. Nine evapotranspiration scenarios were run combining three potential evaporation rates, 0.5 mm/day, 1 mm/day and 2 mm/day, and three potential transpiration rates, 0.5 mm/day, 1 mm/day and 2 mm/day (Table 1).

Potential evaporation and transpiration rates are maintained the same over 100 days after the storm surge event.

Rainfall dilution of soil salt concentration was studied considering different ratios between potential evapotranspiration (ET_p) and rainfall cumulative amounts. First, we fixed evaporation and transpiration rates at 1 mm/day and run 14 scenarios varying ET_p/rainfall ratios between 0.2 and 3 in both sandy loam and clay loam soils. Rainfall events were set every 7 days, for a daily duration, with amounts ranging from 4.5 mm/day to 70 mm/day, corresponding to ET_p/rainfall ratios between 3 and 0.2. Average, final salt soil concentration, root uptake, and concentration decrease after 100 days from the end of the storm surge were compared in the two different soil scenarios. Similar rainfall scenarios were run considering evaporation and transpiration rates of 0.5 mm/day, 0.1 mm/day and 0.01 mm/day in the same soils. Finally, the same analysis was expanded to other three soils, a silty clay loam soil, a silt loam soil, and a sandy soil (Table S1 in Supporting Information S1). From the results obtained, we estimated the time the salt concentration needed to recover 80% of the pre-storm conditions in the root zone, supposing that potential evapotranspiration rates and rainfall remain the same over the recovery time. This approximation is acceptable if both external variables are considered as daily annual averages. The recovery times are calculated using the exponential law $C_f = C_i e^{(-kt)}$, where C_f is the final concentration equal to 80% of the pre-storm initial concentration, C_i is the post-storm concentration, k is the decay factor (1/day) and t is the recovery time (day) (Cartwright et al., 2011; Louvat et al., 1999). All the post-modeling analyses are run in *Rstudio*.

2.4. Field Data

Data collected in a coastal forest in the Delmarva Peninsula (VA) were used to test the results obtained in the model (Figure S2 and TEXT 1 in Supporting Information S1; Nordio & Fagherazzi, 2022). A full description of the data, instruments, and study area can be found in the Supporting Information S1. The effects of rainfall and evapotranspiration on the post-surge water content and electrical conductivity (a proxy for C_i) were studied after three storm surge events occurred between 2019 and 2021: one in October 2019 (Melissa storm), characterized by a water level of 0.86 m on NAVD88, a storm in May 2021, characterized by a water level of 0.72 m and a last storm with water level of 0.59 m on NAVD88. All storm surges were measured at the Wachapreague NOAA station (id: 8631044). Soil water content and electrical conductivity in the 2 months after the storms were analyzed. Electrical conductivity is linked to soil properties, water content, and salt ions concentration. Using extract saturation conductivity variables, we suppose that the increase of conductivity is mostly due to an increase in salt ions concentration.

Rainfall and evapotranspiration data were correlated to the response of the soil moisture at the study site. A weather station located 15 km from the study site is used to collect total radiation, atmospheric pressure, precipitation, and wind characteristics. This weather station is placed in an open area, and we suppose that radiation reaching the instruments is equal to that measured at the top of the canopy. Potential evapotranspiration data were estimated using Penman-Montheith formula at both study sites (Allen. 1998). Net radiation is calculated as 55% of total solar radiation according to Davies (1967), while soil heat flux G is calculated as 10% and 50% of the net radiation respectively during the daylight time and nighttime (Allen, 1998). The crop coefficient for *Pinus taeda* was set to 1, consistent with the values reported for various tree species in Rallo et al., 2021.

Finally, cumulative potential ET and cumulative rainfall over 100 days after the storm surge events were computed and ET/Rainfall ratios calculated. Post-storm surge trends for each of the considered storm surge events were analyzed for both soil salinity and water content over 100 days. The field data were interpreted and discussed according to the ET/Rainfall ratios and compared to model results.

3. Results

3.1. Evapotranspiration Effects on Post-Storm Soil Salinity Conditions

The salinization effect of the storm surge is felt in the entire column of sandy loam soil, while it is limited to the root zone in the clay loam soil. Here, the soil salinity is stratified, with values decreasing from 23 to 10 ppt from 5 to 40 cm below the ground surface. Soil salinity increases in both sandy and clay loam when evaporation and transpiration rates increase from 0 mm/day to 2.5 mm/day (Figures 1a–1d, Figure S3 in Supporting Information S1). Evaporation mostly affects the first 10 cm of soil, while transpiration affects the entire root zone. At 5 cm below the ground surface, a maximum soil salinity of 80 ppt is reached in both sandy loam soil and clay loam soil after 100 days with an average potential evaporation of 2.5 mm/day (Figures 1a–1c). When the potential

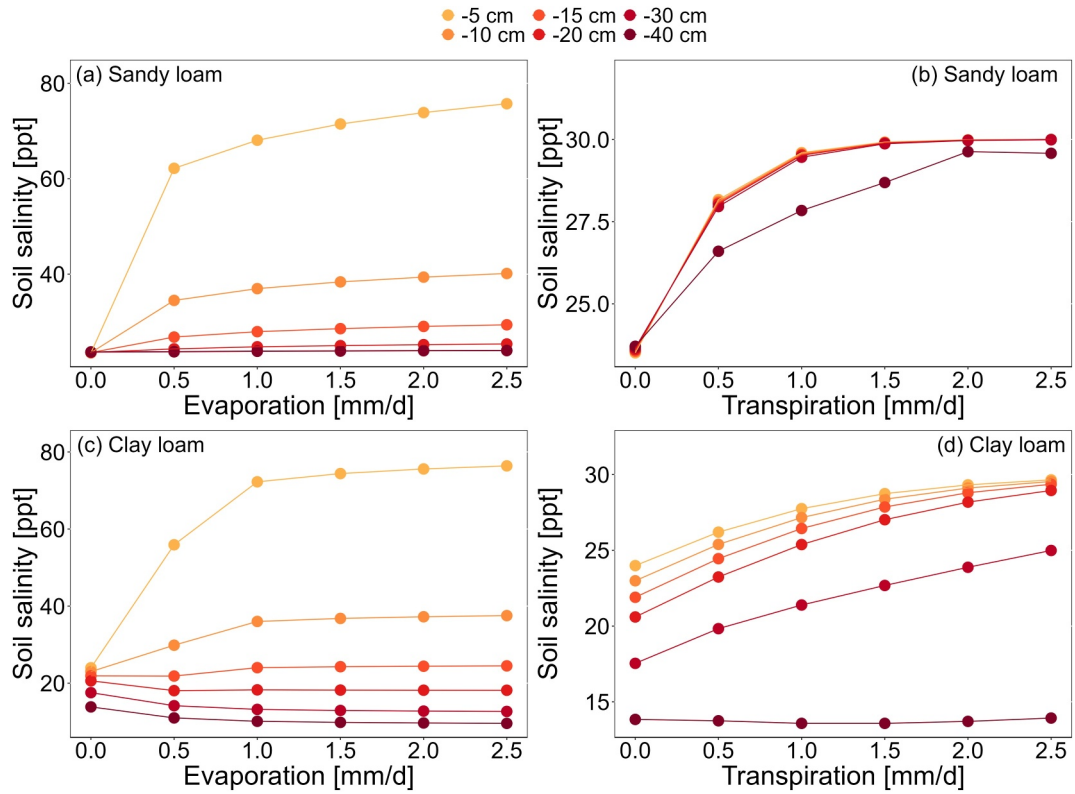

Figure 1. Final concentration of soil salinity 100 days after the storm surge with different constant potential evaporation and transpiration rates in sandy loam (a, b) and clay loam (c, d) soils.

evapotranspiration rates are extremely low (~0), the root zone water content decreases and salt concentration values are reduced by 1.5 ppt in the sandy loam while remain quite constant in the clay loam. Potential transpiration rates of 2.5 mm/day increase the soil salinity in the root zone of around 26% in the sandy loam soil (Figure 1b) and between 47% and 27% in the clay loam soil at respectively 30 and 5 cm below the ground surface (Figure 1d).

3.2. Salinization Effects on Post-Surge Root Water Uptake

Cumulative average root water uptakes in different potential evapotranspiration scenarios are compared in Figure 2. Root water uptake increases as the potential transpiration rates increase. A small difference between root uptake at different evaporation rates is detected in sandy loam soil (Figure 2a). Hundred days after the storm, the cumulative root water uptake reaches average values between 5 and 12 mm respectively for 2 mm/day and 0.5 mm/day potential transpiration scenarios in a sandy loam soil (Figure 2a). In the clay loam soil, the cumulative root uptake is from four to six times higher than in the sandy loam soil. In this case the cumulative root uptake ranges between 20 and 65 mm respectively for potential transpiration rates of 2 mm/day and 0.5 mm/day (Figure 2b). Storm-surge soil salinization uniformly affects the root zone in the sandy loam soil, increasing the initial salt concentration to 25 ppt. In these conditions, root uptake is significantly reduced along the entire root zone length (Figure 2c). In the clay loam soil, the soil salinity stratification is beneficial for tree roots, that can uptake freshwater from deep soil layers (Figure 2d). This is clearly shown at $t = 1$ day in Figure S4 in Supporting Information S1. Moreover, the low permeability of a clay soil helps retaining water (Figure S3 in Supporting Information S1). As a consequence, a slightly higher soil salinity increase is detected in the clay loam soil (Figure 2d).

We compute root uptake for normal soil conditions, where a deficit of oxygen (flooding period) or of water (drying period) cannot be detected and soil salinity is below the threshold that *Pinus taeda* tolerates. In these conditions, trees uptake water according to the maximum potential transpiration rates. The difference between cumulative normal root uptake before the storm surge and root uptake after the surge over 2, 5, 10, 30, 50 and

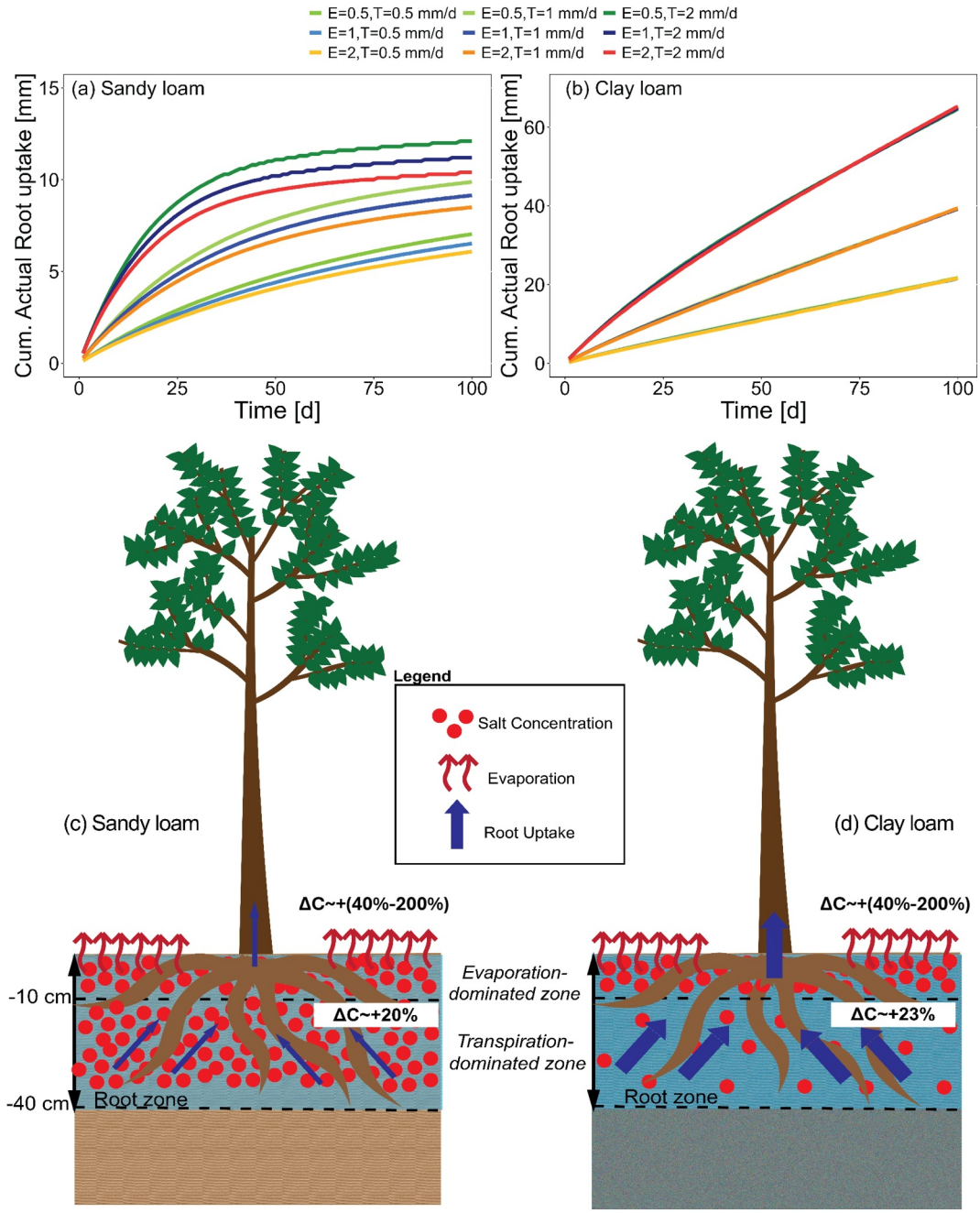

Figure 2. Cumulative root uptake 100 days after the storm surge in sandy loam (a) and clay loam soil (b). Dynamics of soil salinity are summarized for a sandy soil (c) and a clay soil (d). ΔC represents the average increase of salt concentration in the root zone over the 100 days after the storm surge driven by evaporation and transpiration rates.

100 days is shown in Figure 3 (Table 1). The percentage reduction in post-surge root uptake is significantly higher ($p < 0.05$) in sandy loam than in clay loam soil for all the time scales considered. After 100 days, the cumulative decrease in root uptake is on average 90% in sandy loam and 60% in clay loam soils.

3.3. Rainfall Effects on Soil Salinity and Root Water Uptake

As the ET_p/rainfall ratios increases, the soil salinity measured after 100 days also increases (Figure 4a, Figure S5 in Supporting Information S1). Water content in sandy loam soil is half that of clay loam soil due to better drainage (Figure 4b). When ET_p is much higher than the cumulative rainfall, salinity values reach 32 and 25 ppt in

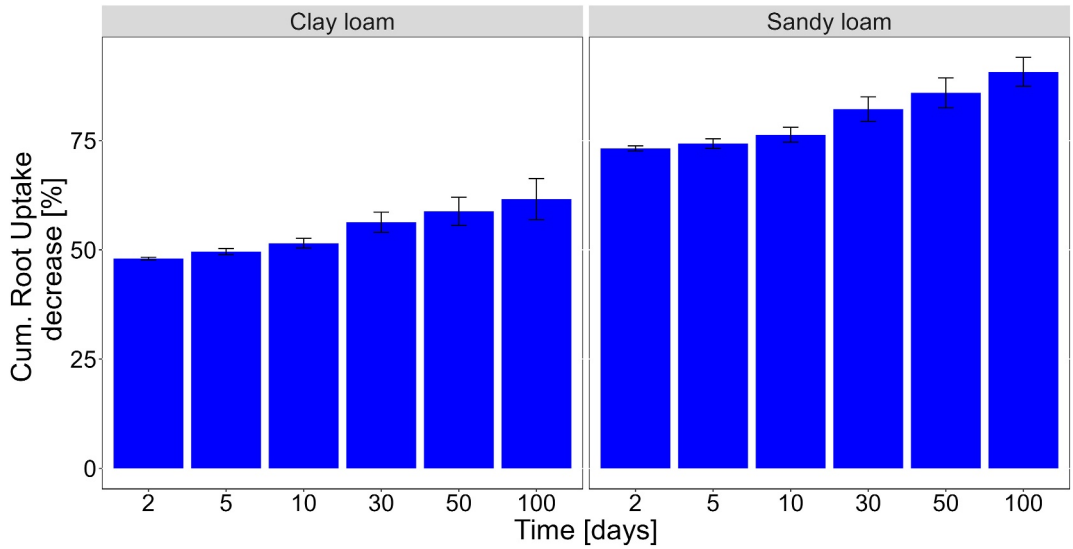

Figure 3. Percentage cumulative root uptake decrease after a storm surge event at different times after the storm surge.

sandy loam soil and clay loam soil respectively. When cumulative rainfall is higher than ET_p (ET_p/Rainfall ratios lower than 1) soil salinity is diluted in sandy loam soils. For instance, for ET_p/Rainfall = 0.5, the final soil salinity is 2 and 7 ppt in sandy and clay loam soils respectively (Figure 4a), and the relative salinity decrease is 90% and 60% (Figure 4c). Once ET_p/Rainfall ratios become higher than 1, evapotranspiration worsens soil salinity conditions in sandy soils. Root uptake in sandy loam and clay loam soils are similar when rainfall amounts are sufficiently higher than cumulative ET_p (Figure 4d). For low rainfall amounts, water uptake is less in sandy loam

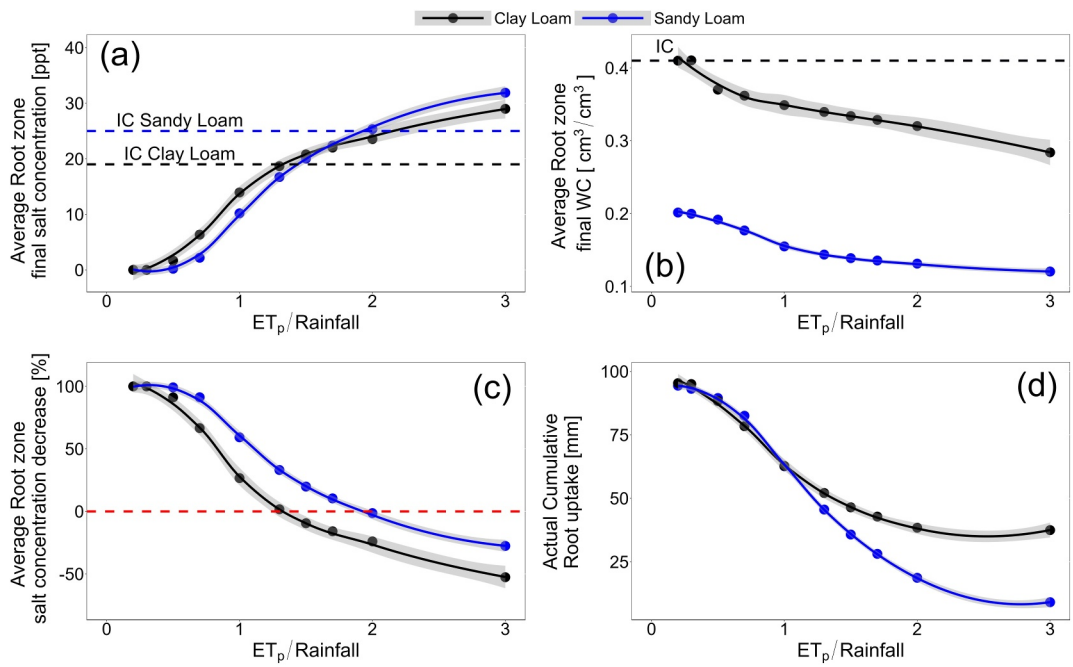

Figure 4. Average final salt concentration (a), final water content (b), concentration decrease (c), and cumulative root uptake (d) in the root zone 100 days after the storm surge for sandy loam and clay loam soils for different ET_p/Rainfall ratios. Filled circles represent the modeling results after 100 days, while the continuous line and the gray area represent respectively the local fitting regression and its confidence interval. The dotted black and blue lines identify the initial conditions for clay loam and sandy soil, respectively. Note: Both soil types start with the same initial water content at saturation. The dotted red line identifies the transition point between salt concentration increase and decrease due to ET_p/Rainfall.

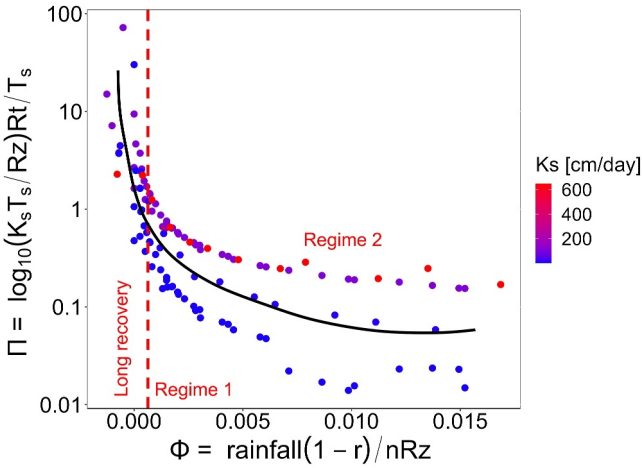

Figure 5. Dimensionless Π–Φ plot identifying recovery time as a function of soil characteristics, ET_p/Rainfall ratios r, and evapotranspiration rates. *Y* axis is in logarithmic scale. Φ represents the potential volume of rainfall infiltrating compared to the volume of pores available in the root zone (Rz) per unit of area adjusted with potential evaporation losses, Π, represents the days soil needs to recover (Rt) compared to simulation time (T_s = 100 days), weighed using the soil saturated hydraulic conductivity K_S. Red dashed line divides the soil salinity recovery in long recovery mainly dependent on soil characteristics with $\phi < 0$ and variable recovery dependent on both soil properties and ET_p/Rainfall ratios for $\phi > 0$. In this latter case, two regimes can be distinguished: Regime 1, for soil with higher saturated hydraulic conductivity and fast recovery and Regime 2, for soils with lower conductivity and longer recovery.

soils, where salinity conditions are worse. For ET_p/Rainfall ratios equal to 3, cumulative root water uptake reaches minimum values at around 20 mm for sandy and 3 mm for clay loam soils (Figure 4d). In Figure S6 in the Supporting Information S1, soil salinity reduction and water content over 100 days are shown at 5 and 30 cm below the ground surface.

3.4. Time to Recover to Pre-Storm Salt Concentration

Time to recover to 80% of the pre-storm salt soil concentration was calculated in each scenario (Table S2, in Supporting Information S1). Time to recover increases as evapotranspiration rates increase. When evapotranspiration rates are significantly higher than rainfall, pre-storm soil salinity conditions are not recovered (Figure S7 in Supporting Information S1). Time to recover (Rt), ET_p/Rainfall ratios (r), cumulative rainfall over 100 days after the storm surge (cumET), root zone depth (Rz = 40 cm) and hydraulic conductivity K_s are used to summarize the external inputs on the post-storm salinity conditions in dimensionless terms (Figure 5). From the Buckingham theorem, two dimensionless groups are derived: $\phi = \frac{Rainfall(1-r)}{nRz}$ represents the potential volume of rainfall that could infiltrate compared to the volume of pores available in the root zone per unit of area adjusted with potential evaporation losses; $\Pi = -\frac{\log_{10}\left(\frac{K_S T_s}{Rz}\right) Rt}{T_s}$ represents the number of days the soil needs to recover compared to the simulation time (T_s = 100 days), weighed using the soil saturated hydraulic conductivity K_S. To obtain a dimensionless parameter and to account for the large range of K_S values (from 1.68 cm/d to 647.9 cm/d), we take the logarithm of K_S multiplied by T_s/Rz.

In Figure 5 we can distinguish three different zones where rainfall, evapotranspiration and soil conductivity regulate soil salinity recovery time. For $\phi < 0$, recovery time will be likely longer than 1 year. For $\phi > 0$, we can distinguish two regimes according to soil conductivity. Regime 1 is characteristic of low-conductivity soils while regime 2 is characteristic of high conductive soils. For the same ϕ, time to recover for soil in regime 1 is much longer than soils in regime 2.

3.5. Study Case: Coastal Forest in Delmarva Peninsula

The effects of rainfall events and evapotranspiration on soil conductivity were studied in a coastal forest in the Delmarva Peninsula, USA (Figure 6 and Figure S8 in Supporting Information S1). We consider two similar storm surges that occurred in October 2019 and October 2021. The surges increased soil conductivity to 15 mS/cm and the water content to 0.1–0.2 cm^3/cm^3 (Figures 6b–6d). Over the next 2 months, the average potential evapotranspiration was estimated around 0.25 mm/hr. Between October and December 2019, cumulative rainfall amount was around 170.52 mm while between October and December 2021, the weather station measured 93.46 mm of rainfall (Figures 6a–6c). Therefore, the ET_p/Rainfall ratios were calculated as 0.92 and 1.96 respectively for the post-storm periods associated to storm surge event in October 2019 and October 2021. After the storm surge in October 2019, soil conductivity decreased due to rainfall (low ET_p/Rainfall). In particular, in the first week after the surge, 70 mm of rainfall reduced the soil conductivity of around 2 ppt. Overall, at the end of December the soil salinity reached values of 17 mS/cm, with a decrease of 30%. A similar trend can be detected over the months after the storm surge of May 2021 (Figure S8b in Supporting Information S1). During this period, the mean potential evapotranspiration and rainfall were respectively estimated around 345.31 and 283.04 mm with a ET/Rainfall ratio of 1.22 (Figure S8a in Supporting Information S1). In the two months following the surge of October 2021, higher evapotranspiration inhibited soil conductivity recovery (Figure 5d). Overall, the soil conductivity increased of 1.5 mS/cm (Figure 5d). Water content decreased over the post-storm surge period because the soil drained due to percolation. The rainfall effects are instantaneously felt as a very small spike in soil water content that dilute soil conductivity, since the soil is close to saturation (Figures 6b–6d). Evapotranspiration and rainfall are important for the long-term soil salinity value after the storm surge event.

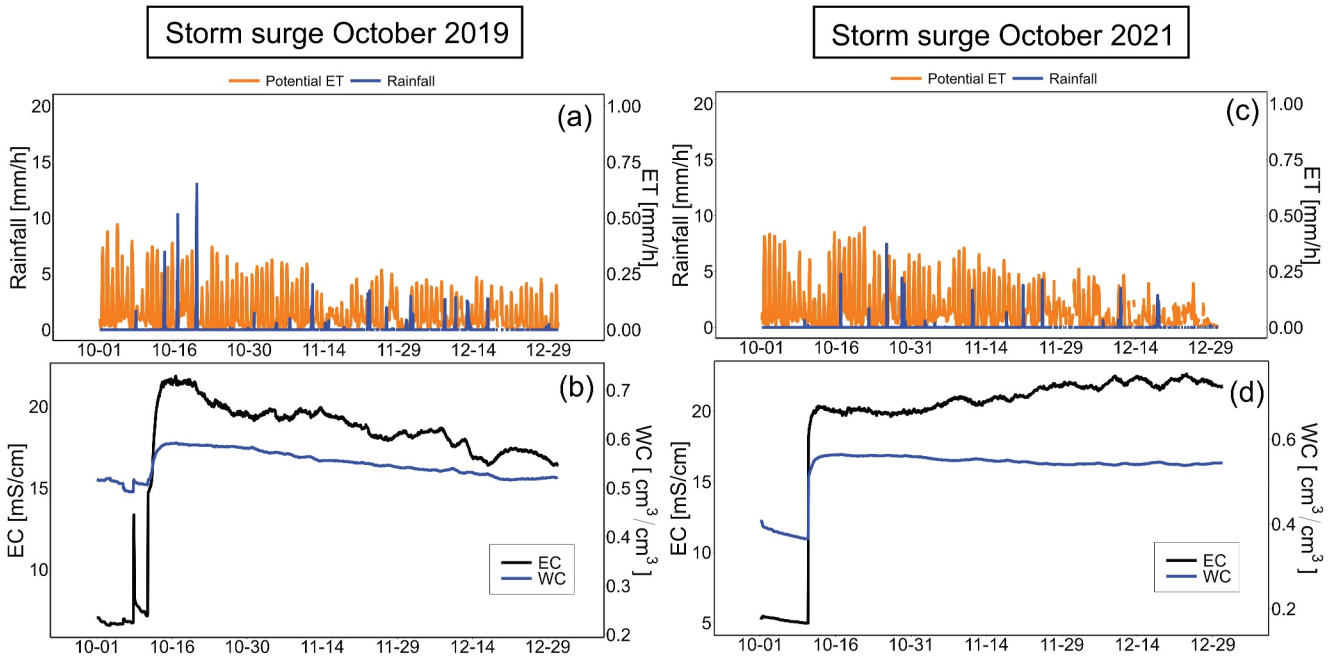

Figure 6. Rainfall and potential evapotranspiration data measured after the storm surges of (a) October 2019 and (c) October 2021. (b, d) Soil water content and conductivity collected in the same period in a forested area in the Delmarva Peninsula, Virginia USA.

4. Discussion

In this study, we shed light on the role of evapotranspiration and rainfall on the recovery of soil salinity in the root zone of a coastal forest after storm surges. In particular, we focused on the vegetation response in terms of transpiration in different soil types, suggesting a beneficial effect of clay loam soil on root uptake. Moreover, evapotranspiration rates higher than rainfall rates augments the post-storm soil salinity. Soil hydrological response is strictly related to edaphic characteristics and has significant consequences for the ecology of coastal vegetation.

4.1. Soil Salinity and Root Uptake Depends on Soil Characteristics

Storm surge events periodically flood coastal vegetated areas, affecting soil moisture and salinity conditions and eventually contaminating groundwater. Previous studies focused on quantifying the effects of storm surge events on groundwater (e.g., Guimond & Michael, 2021; Yang et al., 2018; Yu et al., 2016). These studies estimated the recovery time to pre-storm groundwater conditions as a function of soil characteristics. Few studies focused on evaporation and post-storm salinity conditions. For instance, Yu et al. (2021) used a 2D model to estimate the effects of evaporation after a storm surge event for different soil texture scenarios. They found that in clay and silty soils evaporation increased soil salinity with respect to sandy soils. They estimated maximum soil salinity values of 90 ppt in the first centimeters of soil 300 days after the surge. Potential evaporation rates were fixed at 10 mm/d and the diluting effect of rainfall was not considered. Geng et al. (2016) explored how evaporation induced salt accumulation in the intertidal zone of a beach. In particular, they showed that the upper intertidal beach is less affected by waves and tidal action; as a result, evaporation increased soil salinity in the top 5 cm to 70 ppt. In another work, Geng and Boufadel (2015) discovered that dilution triggered by rainfall decreased soil salinity in a sandy beach. All these studies focused on sandy beaches and not on coastal forests bordering a salt marsh. In coastal forests, the soil can present layers of clay and silt that strongly affect infiltration and evapotranspiration. More importantly, vegetation leads to intense transpiration that can affect salinization differently than evaporation.

The combined effect of evaporation and soil heterogeneity on mixing dynamics in shallow wetland soils was studied in Geng et al. (2023). Their results highlighted the importance of evaporation and local soil heterogeneity

for wetland ecosystem dynamics. Where heterogeneity in the soil is present, mixing solute concentration zones can be recognized.

Our simulations confirm these previous results and add some new insights from an ecological perspective. Storm surge events affect soil water content and salinity as a function of soil type. In clay loam soils, the post-storm salinity is higher than in sandy soils after one season (~100 days). Starting from equal pre-storm conditions, saltwater intrusion triggers soil salinity stratification along the soil column in clay soils, only partially affecting the root zone. Salinization is instead felt equally along the entire soil column in sandy soils, contaminating the groundwater. The soil salinity stratification is beneficial for tree root uptake.

Surface soil salinization was found to be different depending on soil properties in areas characterized by shallow groundwater table, affected by salinity intrusion from below (Gollo et al., 2024). Here a top silty layer promotes the lateral salinity dispersion from a tidal river to inland. Dispersion is not present with a sandy layer. Shah et al. (2011) studied salt accumulation in the root zone under variable climate, groundwater table depth and soil conditions. They suggested that as the groundwater depth decreases (shallow groundwater), the soil salt concentration increases. This is because the hydraulic conductivity increases in wet climate conditions. These findings are in accordance with our results.

Moreover, root uptake in different soils is controlled by soil moisture and salinity. Sandy soils, characterized by higher drainage, lead to water content reduction over time. Therefore, root uptake is reduced in comparison to clay soils, approaching values closer to the wilting point. For high soil salinities, root uptake decreases, and more water remains available in the soil preventing an increase in salt concentration. This dynamic shows soil salinity and root uptake feedback in coastal vegetated areas, enhancing the importance of our results.

4.2. Combined Effect of Evapotranspiration and Rainfall on Recovery Time

When evapotranspiration is dominant with respect to rainfall, root uptake in clay soils is reduced but still much higher than in sandy soils. External rainfall inputs are essential for salinity recovery to pre-storm conditions. Previous studies estimated groundwater recovery from field measurements (Nordio et al., 2023; Terry & Falkland, 2010; Van Biersel et al., 2007) or from models with a fixed net external recharge computed as a difference between precipitation and evapotranspiration (Song et al., 2022; Xiao et al., 2019). For instance, it takes 8 years for a lower-permeability surficial aquifer to recover from flooding caused by a Category 5 hurricane (Xiao et al., 2019). Salinization triggered by hurricanes Katrina and Rita persisted until 10 months after landfall in the groundwater system of coastal Louisiana (Van Biersel et al., 2007). Here we mostly concentrate on the root zone, estimating soil salinity recovery time to pre-storm values. Evaporation, transpiration, and rainfall are set as independent controlling variables. Their actual values are regulated by the hydrological soil conditions and vice versa. Similar to groundwater recovery, soil salinity recovery in the root zone is much faster in sandy soils than in low-permeability soils. According to our results, when soils are characterized by high hydraulic conductivities and low evapotranspiration rates recovery is completed after 1 year. Rainfall events, when post-storm soil water content is low enough to let external water infiltrate, are essential to dilute soil salinity. As climate changes, rainfall events can become more intense or less frequent. These changes can be crucial for soil salinity and consequently local ecology. Dasgupta et al. (2015) predicted that soil salinity will increase by 39.2% across 41 monitoring stations in Bangladesh by 2050, causing significant impacts on local agriculture and the economy. Moreover, sea level rise is going to worsen salinity conditions in the same region.

Soil-salinity recovery time must be compared to the return period of storm surges. If the return period of the storm surge event is long enough, soil salinity can fully recover before the subsequent surge. Storm surge events characterized by different return periods often flood the coast, keeping soil salinity high. When soils consist of fine material, soil salinity recovery does not usually occur before another storm surge floods the area. Nordio et al. (2023) showed that medium storm surge events, with return period of around 2 years, can have an impact as significant as the strongest hurricanes in clay soils. This is because the high temporal frequency does not often allow a complete recovery, and salinity values are maintained higher than the threshold tolerated by in-situ vegetation, irreversibly affecting their normal physiological functions.

4.3. Ecological Implications

Feedback between tree root uptake and salt infiltration are crucial in coastal areas affected by sea level rise and storm surge events. Moderate salt tolerant tree species can survive if soil salinity is lower than a fixed threshold and if water content guarantees roots oxygen supply (Poulter et al., 2008). For instance, *Pinus taeda*, the dominant species at our study site, can better survive at soil salinity values lower than 5 ppt (Pezeshki, 1992). If the recovery time to pre-storm soil conditions is too long, roots suffocate, tree photosynthetic activity slows, and canopies show clear signs of stress (McDowell et al., 2022; Munns & Tester, 2008; Woods et al., 2020). Frequent salinization events kill trees, even in soils with high hydraulic conductivity where recovery time is fast (Barlow & Reichard, 2010).

Salinity and flooding events are detrimental for forest survival, reducing root conductance and eventually causing root mortality. Under these stressed conditions plants react to the reduced water uptake (due to lower gradient between soil and canopy) through stomatal closure. This reduces the photosynthetic activity and the CO_2 assimilation from the atmosphere, leading to carbon starvation (Choat et al., 2018; McDowell et al., 2022; Wang et al., 2022). If the photosynthetic activity rate is slow, the photosynthetic capacity is no longer able to supply the carbohydrate requirements of young leaves. Forest loss is a major issue for society, since trees are a main source of carbon sequestration in terrestrial environments. Coastal forest retreat driven by climate change adds to the already known causes of forest decline as deforestation, wildfires, and droughts.

Along the coast, carbon sequestration and storage are mainly regulated by seagrasses, marshes, and coastal forests. Recent work in ghost forests, where dead tree stands coexist with invasive vegetation, has estimated large declines in aboveground carbon associated with tree mortality, suggesting that forest retreat and marsh expansion may encourage large net carbon emissions. In fact, biomass mortality in the forest will not be offset in the short term by an increase in soil carbon sequestration of the encroaching marsh, converting the coastal area to a net carbon source (Kirwan et al., 2023; Warnell et al., 2022). Valentine et al. (2023) estimated that at intermediate rates of sea level rise (∼10 mm/y) landscape connectivity, carbon accumulation rates, and landscape-scale carbon stocks peak. As rates of sea level rise increase, they noted a clear shift from a forest-carbon dominated system, where carbon is mostly stored as woody biomass, to a marsh-carbon dominated system, where around 50% of the carbon is stored in the soil. This soil carbon is considered more labile and might be remobilized in the future.

Our results suggest that trees are healthier in clay or silty soils, due to the combined effects of low saltwater infiltration and salinity stratification in the root zone. Previous studies indicated that clay soils better retain nutrients, since leaching and groundwater contamination can cause severe environmental issues in sandy soils (Barlow & Reichard, 2010; Huang & Hartemink, 2020; Tahir & Marschner, 2017; Uchida, 2000).

In clay soils the low permeability maintains the water content above the wilting point, allowing root uptake during dry periods. On the other hand, the beneficial role of finer soils is thwarted by the limited capacity to store additional freshwater during rainfall events and because they retain salinity for longer, potentially causing negative effects on root activity. However, the long recovery time of soils with low permeability is counterbalanced by the post-storm salinity stratification along the soil depth. Soil salinity stratification can be beneficial for roots, since it can partially protect them from saltwater intrusion. For example, moderately salt tolerant tree species can uptake water from the deep layers, where salinity values are low. From our results we conclude that clay layers act like beneficial barriers, buffering the salinity infiltration through the root zone and protecting groundwater from salinity contamination. As a result, forest retreat can be delayed in clay soils.

The ratio between evapotranspiration and rainfall is essential in determining whether soil salinity will recover or not. A high evapotranspiration rate exacerbates soil salinization after a storm surge. In particular, the first soil centimeters below the ground surface are the most affected by evaporation, and can reach extremely high salinity values, preventing roots from uptaking water at these depths. Data collected during fieldwork campaigns in a clay soil show that, when evapotranspiration is significantly higher than rainfall, recovery is not possible.

Scenarios considering only evaporation are likely representative of coastal vegetated areas where trees are stressed, with limited photosynthetic activity. In these conditions transpiration is low and evaporation increases soil salinity in the top soil layers, encouraging the establishment of salt-tolerant grasses (Woods et al., 2020).

Climate change will cause a significant acceleration in sea level rise, more frequent storm surges (Dasgupta et al., 2009; Lin et al., 2012), warmer temperatures, and possibly an increase in return period of rainfall events

(Dasgupta et al., 2015). Moreover, according to Hassani et al. (2021), soil salinity in the top-soil layers of coastal regions is predicted to increase due to dry deposition of sea salt (aeolian processes). In the southern United States, daily dry salt deposition has increased of 1 mg/(d m^2) between 1961 and 1990 and it is projected to increase to 7.7 mg/(d m^2) between 1971 and 2100.

4.4. Model Limitations and Future Improvements

Our results shed light on water-plants feedbacks in the root zone, suggesting different root-uptake rates depending on soil characteristics. Using a 1D model, we expand the results already presented in the literature (Geng et al., 2016, 2023; Yu et al., 2021) by adding the impact of transpiration on soil salinity and the beneficial effect of clay layers for root uptake.

Our simplified approach enabled us to isolate key dynamics. More complex models could in the future address some shortcomings of our approach. For example, HYDRUS 1D is a constant density model. In coastal groundwater systems, where salinity can affect water density, this simplification can result in altered outcomes. More complete 2D models are generally preferred when the focus is on groundwater contamination (e.g., Paldor & Michael, 2021; Yang et al., 2018). Several studies focused on variable-density flow in saturated porous media (Diersch & Kolditz, 2002; Simmons, 2005; Simmons et al., 2010; Werner et al., 2013) since the effect of density variations is much more significant in the saturated zone (Younes et al., 2022). Here we focus instead on the unsaturated root zone. In the unsaturated zone, the density variation in the liquid phase is less important than the density variation between the liquid and the air phase (about three orders of magnitude). Liu et al. (2015) and Simmons (2005) showed that gravity flow and not density-driven flow is dominant in the unsaturated zone. Constant-density approaches were also adopted in Zeng et al. (2014) and Li et al. (2010) to study salt leaching in irrigation scenarios using HYDRUS1D.

To analyze the post-surge dynamics we derived soil salinity and water content distribution along the depth from a storm surge simulation. As it was beyond our scope, we selected only one storm surge scenario, without accounting for the possible effect of different storm surges on salinity distribution. Although additional analyses could be conducted considering various storm surge categories, we believe that salinity stratification in clay soil would persist regardless of the storm surge scale, unlike in sandy soil (e.g., Yu et al., 2021). This is further confirmed by Nordio, Pratt, et al. (2024), where the impacts of storm surges on vertical salinity distribution were analyzed under various storm surge characteristics and initial soil condition scenarios, considering both clay and sandy soils. Nonetheless, a more comprehensive investigation into the impact of storm surge scale on initial conditions is necessary to accurately quantify ecological response.

Potential evaporation and transpiration rates were kept constant over the entire period of simulation, although effective rates changed as a function of edaphic conditions. These potential rates were considered as mean daily seasonal values and depending on external climatic conditions. Hourly variable evaporation rates were considered in Geng et al. (2016), where they studied a post-surge salinity increase driven by evaporation in an intertidal sandy beach. An hourly analysis of evapotranspiration in vegetated areas could detect the response at short timescales, with maximum daily rates and limited nighttime response, but would not substantially change the results of long-term simulations like those presented herein.

Potential root uptake was supposed to be constant along the root zone depth and identical in sandy and clay soils. This simplification reflects the fact that 70% of active roots are located in the first 40 cm on the unsaturated zone (Mou et al., 1995; Parker & Lear, 1996; Xu et al., 2016). To estimate root distribution and the root uptake contribution at different depths is difficult, and results are usually local and difficult to generalize (Giambastiani et la. 2022).

We also considered homogenous soil columns. Despite the common occurrence of soil layering and vertical textural contrast in coastal environments, their impact on coastal processes is often overlooked (Holland & Elmore, 2008). For example, a sandy layer overlying finer material can inhibit upward water movement, preventing it from reaching the surface, unlike in silty soils (Saxton et al., 1986). In the presence of vertical textural differences, greater evaporative losses have been quantified compared to homogeneous soil conditions, with consequences for water and salinity distributions (Lehmann & Or, 2009). Heterogeneity in the soil can also create hotspots of salinity (Geng et al., 2023), that could affect ecological responses. Moreover, the complex interactions between clay particles and solute ions were not considered in our simplified analysis. Clay particles, which are

negatively charged due to isomorphous displacement, attract positive ions (e.g., Na^+). These ions tend to diffuse away from the surface to the bulk solution where their concentration is lower (Luckham & Rossi, 1999). This phenomenon is known as electrical double layer (EDL). As the concentration of Na^+ increases, the EDL size decreases, leading to clay particle aggregation (Rengasamy and Marchuk, 2011), cracks, and consequently increased hydraulic conductivity (Felhendler et al., 1974). Evaporation also contributes to crack formation when soil water content decreases and the clay structure shrinks. When the NaCl concentration is higher, the evaporation rate decreases, affecting soil water content, crack distribution, and dimensions. Specifically, for high NaCl concentrations, the crack ratio, fractal dimension, crack width, and crack density decrease (DeCarlo & Shokri, 2014; Li et al., 2021; Shokri et al., 2015; Zhang et al., 2017). Crack formation impacts soil structure by creating preferential pathways for water flow and solute dispersion, similar to the presence of macropores, dead root systems, or fractured rocks (Li et al., 2016; Nimmo, 2021).

This notwithstanding, we believe that our simplified model can provide significant insight on edaphic conditions after storm surges. Our results are important for the survival of coastal forests, and can inspire more sophisticated ecohydrological studies in similar environments.

5. Conclusions

Our analysis suggests that rainfall and evapotranspiration can significantly affect soil salinity after a storm surge and the recovery time to pre-storm conditions. In particular, our modeling results shed light on the post-surge dynamics in different types of soil. Storm surge salinization of clay soils results in soil salinity stratification in the root zone. This is beneficial for roots, since they can uptake freshwater from deeper layers. As a result, root uptakes can be between 4 and 5 times higher than in sandy soils, where salinity after storm events reaches the groundwater homogenizing the entire soil column. Moreover, root uptakes 100 days after the storm surge are reduced by 90% in a sandy loam soil and only by 60% in a clay loam soil. When cumulative rainfall is significantly higher than cumulative evapotranspiration (low ET_p/Rainfall ratios) soil salinity recovery is encouraged. On average, in the root zone of sandy soils dilution due to rainfall is between 20% and 50% higher than in clay soils. As a consequence, recovery times are shorter. For high ET_p/Rainfall ratios, vegetation in clay soils can survive better, due to the compounding effects of soil salinity stratification and low permeability, which maintains water content closer to wilting point.

Data Availability Statement

Data supporting findings of this research are openly available in the LTER-VCR (Long Term Ecological Research -Virginia Coast Reserve) website (Fagherazzi & Nordio, 2023).

Acknowledgments
This research was funded by the USA National Science Foundation awards 1832221 (VCR LTER), 2224608 (PIE LTER), and 2012322 (CZN Coastal Critical Zone).

References

Allen, J. L., & Lendemer, J. C. (2016). Quantifying the impacts of sea-level rise on coastal biodiversity: A case study on lichens in the mid-Atlantic coast of eastern North America. *Biological Conservation*, *202*, 119–126. https://doi.org/10.1016/j.biocon.2016.08.031

Allen, R. G. (1998). Crop evapotranspiration. *Fao Irrigation and Drainage Paper*, *56*, 60.

Aragüés, R., Medina, E. T., Martínez-Cob, A., & Faci, J. (2014). Effects of deficit irrigation strategies on soil salinization and sodification in a semiarid drip-irrigated peach orchard. *Agricultural Water Management*, *142*, 1–9. https://doi.org/10.1016/j.agwat.2014.04.004

Barlow, P. M., & Reichard, E. G. (2010). Saltwater intrusion in coastal regions of North America. *Hydrogeology Journal*, *18*(1), 247–260. https://doi.org/10.1007/s10040-009-0514-3

Befus, K. M., Barnard, P. L., Hoover, D. J., Finzi Hart, J. A., & Voss, C. I. (2020). Increasing threat of coastal groundwater hazards from sea-level rise in California. *Nature Climate Change*, *10*(10), 946–952. https://doi.org/10.1038/s41558-020-0874-1

Burkett, V. R., Nicholls, R. J., Fernandez, L., & Woodroffe, C. D. (2008). Climate change impacts on coastal biodiversity.

Cantelon, J. A., Guimond, J. A., Robinson, C. E., Michael, H. A., & Kurylyk, B. L. (2022). Vertical saltwater intrusion in coastal aquifers driven by episodic flooding: A review. *Water Resources Research*, *58*(11), e2022WR032614. https://doi.org/10.1029/2022wr032614

Cardenas, M. B., Bennett, P. C., Zamora, P. B., Befus, K. M., Rodolfo, R. S., Cabria, H. B., & Lapus, M. R. (2015). Devastation of aquifers from tsunami-like storm surge by Supertyphoon Haiyan. *Geophysical Research Letters*, *42*(8), 2844–2851. Craine, S. I., & Orians, C. M. (2006). Effects of flooding on pitch pine (Pinus rigida Mill.) growth and survivorship. The Journal of the Torrey Botanical Society, 289-296. https://doi.org/10.1002/2015gl063418

Carr, J., Guntenspergen, G., & Kirwan, M. (2020). Modeling marsh-forest boundary transgression in response to storms and sea-level rise. *Geophysical Research Letters*, *47*(17), e2020GL088998. https://doi.org/10.1029/2020gl088998

Cartwright, I., Hofmann, H., Sirianos, M. A., Weaver, T. R., & Simmons, C. T. (2011). Geochemical and 222Rn constraints on baseflow to the Murray River, Australia, and timescales for the decay of low-salinity groundwater lenses. *Journal of Hydrology*, *405*(3–4), 333–343. https://doi.org/10.1016/j.jhydrol.2011.05.030

Celia, M. A., Bouloutas, E. T., & Zarba, R. L. (1990). A general mass-conservative numerical solution for the unsaturated flow equation. *Water Resources Research*, *26*(7), 1483–1496. https://doi.org/10.1029/wr026i007p01483

Choat, B., Brodribb, T. J., Brodersen, C. R., Duursma, R. A., López, R., & Medlyn, B. E. (2018). Triggers of tree mortality under drought. *Nature*, *558*(7711), 531–539. https://doi.org/10.1038/s41586-018-0240-x

Dasgupta, S., Hossain, M. M., Huq, M., & Wheeler, D. (2015). Climate change and soil salinity: The case of coastal Bangladesh. *Ambio*, *44*(8), 815–826. https://doi.org/10.1007/s13280-015-0681-5

Dasgupta, S., Laplante, B., Murray, S., & Wheeler, D. (2009). *Climate change and the future impacts of storm-surge disasters in developing countries* (Vol. 182). Center for Global Development Working Paper.

Davies, J. (1967). A note on the relationship between net radiation and solar radiation. *Quarterly Journal of the Royal Meteorological Society*, *93*(395), 109–115. https://doi.org/10.1002/qj.49709339511

DeCarlo, K. F., & Shokri, N. (2014). Salinity effects on cracking morphology and dynamics in 3-D desiccating clays. *Water Resources Research*, *50*(4), 3052–3072. https://doi.org/10.1002/2013wr014424

de Melo, M. L. A., & van Lier, Q. D. J. (2021). Revisiting the Feddes reduction function for modeling root water uptake and crop transpiration. *Journal of Hydrology*, *603*, 126952. https://doi.org/10.1016/j.jhydrol.2021.126952

Diersch, H. J., & Kolditz, O. (2002). Variable-density flow and transport in porous media: Approaches and challenges. *Advances in Water Resources*, *25*(8–12), 899–944. https://doi.org/10.1016/s0309-1708(02)00063-5

Doyle, T. W., Krauss, K. W., Conner, W. H., & From, A. S. (2010). Predicting the retreat and migration of tidal forests along the northern Gulf of Mexico under sea-level rise. *Forest Ecology and Management*, *259*(4), 770–777. https://doi.org/10.1016/j.foreco.2009.10.023

Fagherazzi, S., Anisfeld, S. C., Blum, L. K., Long, E. V., Feagin, R. A., Fernandes, A., et al. (2019). Sea level rise and the dynamics of the marsh-upland boundary. *Frontiers in Environmental Science*, *7*. https://doi.org/10.3389/fenvs.2019.00025

Fagherazzi, S., & Nordio, G. (2023). Groundwater, soil moisture, light and weather data in Brownsville forest, Nassawadox, VA, 2019-2023 [Dataset]. *Virginia Coast Reserve Long-Term Ecological Research Project Data Publication knb-lter-vcr.349.5*. https://doi.org/10.6073/pasta/09605b9c54b3fb809f78043f7872fe00

Fan, Y., Li, H., & Miguez-Macho, G. (2013). Global patterns of groundwater table depth. *Science*, *339*(6122), 940–943. https://doi.org/10.1126/science.1229881

Felhendler, R., Schainberg, I., & Frenkel, H. (1974). Dispersion and the hydraulic conductivity of soils in mixed solutions.

Fernandes, A., Rollinson, C. R., Kearney, W. S., Dietze, M. C., & Fagherazzi, S. (2018). Declining radial growth response of coastal forests to hurricanes and nor'easters. *Journal of Geophysical Research: Biogeosciences*, *123*(3), 832–849. https://doi.org/10.1002/2017jg004125

Geng, X., & Boufadel, M. C. (2015). Impacts of evaporation on subsurface flow and salt accumulation in a tidally influenced beach. *Water Resources Research*, *51*(7), 5547–5565. https://doi.org/10.1002/2015wr016886

Geng, X., & Boufadel, M. C. (2017). The influence of evaporation and rainfall on supratidal groundwater dynamics and salinity structure in a sandy beach. *Water Resources Research*, *53*(7), 6218–6238. https://doi.org/10.1002/2016wr020344

Geng, X., Boufadel, M. C., & Jackson, N. L. (2016). Evidence of salt accumulation in beach intertidal zone due to evaporation. *Scientific Reports*, *6*(1), 1–5. https://doi.org/10.1038/srep31486

Geng, X., Boufadel, M. C., Li, H., Na Nagara, V., & Lee, K. (2023). Impacts of evaporation-induced groundwater upwelling on mixing dynamics in shallow wetlands. *Geophysical Research Letters*, *50*(15), e2023GL104642. https://doi.org/10.1029/2023gl104642

Geng, X., Khalil, C. A., Prince, R. C., Lee, K., An, C., & Boufadel, M. C. (2021). Hypersaline pore water in Gulf of Mexico beaches prevented efficient biodegradation of Deepwater Horizon beached oil. *Environmental Science and Technology*, *55*(20), 13792–13801. https://doi.org/10.1021/acs.est.1c02760

Giambastiani, Y., Errico, A., Preti, F., Guastini, E., & Censini, G. (2022). Indirect root distribution characterization using electrical resistivity tomography in different soil conditions. *Urban Forestry and Urban Greening*, *67*, 127442. https://doi.org/10.1016/j.ufug.2021.127442

Gleeson, T., Marklund, L., Smith, L., & Manning, A. H. (2011). Classifying the water table at regional to continental scales. *Geophysical Research Letters*, *38*(5). https://doi.org/10.1029/2010gl046427

Gollo, V. S., Sahimi, M., González, E., Hajati, M. C., Elbracht, J., Fröhle, P., & Shokri, N. (2024). Soil salinization due to saltwater intrusion in coastal regions: The role of soil characteristics and heterogeneity. *InterPore Journal*, *1*(1), ipj2604246. https://doi.org/10.69631/ipj.v1i1nr15

Guimond, J. A., & Michael, H. A. (2021). Effects of marsh migration on flooding, saltwater intrusion, and crop yield in coastal agricultural land subject to storm surge inundation. *Water Resources Research*, *57*(2), e2020WR028326. https://doi.org/10.1029/2020wr028326

Hassani, A., Azapagic, A., & Shokri, N. (2021). Global predictions of primary soil salinization under changing climate in the 21st century. *Nature Communications*, *12*(1), 6663. https://doi.org/10.1038/s41467-021-26907-3

Holland, K. T., & Elmore, P. A. (2008). A review of heterogeneous sediments in coastal environments. *Earth-Science Reviews*, *89*(3–4), 116–134. https://doi.org/10.1016/j.earscirev.2008.03.003

Huang, J., & Hartemink, A. E. (2020). Soil and environmental issues in sandy soils. *Earth-Science Reviews*, *208*, 103295. https://doi.org/10.1016/j.earscirev.2020.103295

Kearney, W. S., Fernandes, A., & Fagherazzi, S. (2019). Sea-level rise and storm surges structure coastal forests into persistence and regeneration niches. *PLoS One*, *14*(5), e0215977. https://doi.org/10.1371/journal.pone.0215977

Kirwan, M. L., & Gedan, K. B. (2019). Sea-level driven land conversion and the formation of ghost forests. *Nature Climate Change*, *9*(6), 450–457. https://doi.org/10.1038/s41558-019-0488-7

Kirwan, M. L., Megonigal, J. P., Noyce, G. L., & Smith, A. J. (2023). Geomorphic and ecological constraints on the coastal carbon sink. *Nature Reviews Earth and Environment*, *4*(6), 393–406. https://doi.org/10.1038/s43017-023-00429-6

Konar, M., Todd, M. J., Muneepeerakul, R., Rinaldo, A., & Rodriguez-Iturbe, I. (2013). Hydrology as a driver of biodiversity: Controls on carrying capacity, niche formation, and dispersal. *Advances in Water Resources*, *51*, 317–325. https://doi.org/10.1016/j.advwatres.2012.02.009

Lehmann, P., & Or, D. (2009). Evaporation and capillary coupling across vertical textural contrasts in porous media. *Physical Review E: Statistical, Nonlinear, and Soft Matter Physics*, *80*(4), 046318. https://doi.org/10.1103/physreve.80.046318

Li, D., Yang, B., Yang, C., Zhang, Z., & Hu, M. (2021). Effects of salt content on desiccation cracks in the clay. *Environmental Earth Sciences*, *80*(19), 1–13. https://doi.org/10.1007/s12665-021-09987-8

Li, J. H., Li, L., Chen, R., & Li, D. Q. (2016). Cracking and vertical preferential flow through landfill clay liners. *Engineering Geology*, *206*, 33–41. https://doi.org/10.1016/j.enggeo.2016.03.006

Li, L., Shi, H., Wang, C., & Liu, H. (2010). Simulation of water and salt transport of uncultivated land in Hetao Irrigation District in Inner Mongolia. *Transactions of the Chinese Society of Agricultural Engineering*, *26*(1), 31–35.

Li, Y., Šimůnek, J., Jing, L., Zhang, Z., & Ni, L. (2014). Evaluation of water movement and water losses in a direct-seeded-rice field experiment using Hydrus-1D. *Agricultural Water Management*, *142*, 38–46. https://doi.org/10.1016/j.agwat.2014.04.021

Lin, N., Emanuel, K., Oppenheimer, M., & Vanmarcke, E. (2012). Physically based assessment of hurricane surge threat under climate change. *Nature Climate Change*, *2*(6), 462–467. https://doi.org/10.1038/nclimate1389

Liu, Y., Kuang, X., Jiao, J. J., & Li, J. (2015). Numerical study of variable-density flow and transport in unsaturated–saturated porous media. *Journal of Contaminant Hydrology*, *182*, 117–130. https://doi.org/10.1016/j.jconhyd.2015.09.001

Louvat, D., Michelot, J. L., & Aranyossy, J. F. (1999). Origin and residence time of salinity in the Äspö groundwater system. *Applied Geochemistry*, *14*(7), 917–925. https://doi.org/10.1016/s0883-2927(99)00026-8

Luckham, P. F., & Rossi, S. (1999). The colloidal and rheological properties of bentonite suspensions. *Advances in Colloid and Interface Science*, *82*(1–3), 43–92. https://doi.org/10.1016/s0001-8686(99)00005-6

Maas, E. V. (1990). Crop salt tolerance. In *Agricultural Salinity Assessment and Management Manual* (pp. 262–304).

May, C. (2020). Rising groundwater and sea-level rise. *Nature Climate Change*, *10*(10), 889–890. https://doi.org/10.1038/s41558-020-0886-x

McDowell, N. G., Ball, M., Bond-Lamberty, B., Kirwan, M. L., Krauss, K. W., Megonigal, J. P., et al. (2022). Processes and mechanisms of coastal woody-plant mortality. *Global Change Biology*, *28*(20), 5881–5900. https://doi.org/10.1111/gcb.16297

Michael, H. A., Russoniello, C. J., & Byron, L. A. (2013). Global assessment of vulnerability to sea-level rise in topography-limited and recharge-limited coastal groundwater systems. *Water Resources Research*, *49*(4), 2228–2240. https://doi.org/10.1002/wrcr.20213

Mou, P., Jones, R. H., Mitchell, R. J., & Zutter, B. (1995). Spatial distribution of roots in sweetgum and loblolly pine monocultures and relations with above-ground biomass and soil nutrients. *Functional Ecology*, *9*(4), 689–699. https://doi.org/10.2307/2390162

Munns, R., & Tester, M. (2008). Mechanisms of salinity tolerance. *Annual Review of Plant Biology*, *59*(1), 651–681. https://doi.org/10.1146/annurev.arplant.59.032607.092911

Nachshon, U. (2018). Cropland soil salinization and associated hydrology: Trends, processes and examples. *Water*, *10*(8), 1030. https://doi.org/10.3390/w10081030

Nimmo, J. R. (2021). The processes of preferential flow in the unsaturated zone. *Soil Science Society of America Journal*, *85*(1), 1–27. https://doi.org/10.1002/saj2.20143

Nordio, G., & Fagherazzi, S. (2022). Groundwater, soil moisture, light and weather data collected in a coastal forest bordering a salt marsh in the Delmarva Peninsula (VA). *Data in Brief*, *45*, 108584. https://doi.org/10.1016/j.dib.2022.108584

Nordio, G., Frederiks, R., Hingst, M., Carr, J., Kirwan, M., Gedan, K., et al. (2023). Frequent storm surges affect the groundwater of coastal ecosystems. *Geophysical Research Letters*, *50*(1), e2022GL100191. https://doi.org/10.1029/2022gl100191

Nordio, G., Gedan, K., & Fagherazzi, S. (2024). Storm surges and sea level rise cluster hydrological variables across a coastal forest bordering a salt marsh. *Water Resources Research*, *60*(2), e2022WR033931. https://doi.org/10.1029/2022wr033931

Nordio, G., Pratt, D., Michael, H. A., & Fagherazzi, S. (2024). Initial soil moisture and soil texture control the impact of storm surges in coastal forests. *The Science of the Total Environment*, *953*, 175911. https://doi.org/10.1016/j.scitotenv.2024.175911

Paldor, A., & Michael, H. A. (2021). Storm surges cause simultaneous salinization and freshening of coastal aquifers, exacerbated by climate change. *Water Resources Research*, *57*(5), e2020WR029213. https://doi.org/10.1029/2020wr029213

Parker, M. M., & Van Lear, D. H. (1996). Soil heterogeneity and root distribution of mature loblolly pine stands in piedmont soils. *Soil Science Society of America Journal*, *60*(6), 1920–1925. https://doi.org/10.2136/sssaj1996.03615995006000060043x

Pezeshki, S. R. (1992). Response of Pinus taeda L to soil flooding and salinity. In *Annales des Sciences Forestières*, (Vol. 49, No. (2), pp. 149–159). EDP Sciences. https://doi.org/10.1051/forest:19920205

Pezeshki, S. R., DeLaune, R. D., & Anderson, P. H. (1999). Effect of flooding on elemental uptake and biomass allocation in seedlings of three bottomland tree species. *Journal of Plant Nutrition*, *22*(9), 1481–1494. https://doi.org/10.1080/01904169909365729

Poulter, B., Christensen, N. L., & Qian, S. S. (2008). Tolerance of Pinus taeda and Pinus serotina to low salinity and flooding: Implications for equilibrium vegetation dynamics. *Journal of Vegetation Science*, *19*(1), 15–22. https://doi.org/10.3170/2007-8-18410

Rabbel, I., Bogena, H., Neuwirth, B., & Diekkrüger, B. (2018). Using sap flow data to parameterize the Feddes water stress model for Norway spruce. *Water*, *10*(3), 279. https://doi.org/10.3390/w10030279

Rajmohan, N., Masoud, M. H., & Niyazi, B. A. (2021). Impact of evaporation on groundwater salinity in the arid coastal aquifer, Western Saudi Arabia. *Catena*, *196*, 104864. https://doi.org/10.1016/j.catena.2020.104864

Rallo, G., Paço, T. A., Paredes, P., Puig-Sirera, À., Massai, R., Provenzano, G., & Pereira, L. S. (2021). Updated single and dual crop coefficients for tree and vine fruit crops. *Agricultural Water Management*, *250*, 106645. https://doi.org/10.1016/j.agwat.2020.106645

Rengasamy, P., Chittleborough, D., & Helyar, K. (2003). Root-zone constraints and plant-based solutions for dryland salinity. *Plant and Soil*, *257*(2), 249–260. https://doi.org/10.1023/a:1027326424022

Rengasamy, P., & Marchuk, A. (2011). Cation ratio of soil structural stability (CROSS). *Soil Research*, *49*(3), 280–285. https://doi.org/10.1071/sr10105

Rotzoll, K., & Fletcher, C. H. (2013). Assessment of groundwater inundation as a consequence of sea-level rise. *Nature Climate Change*, *3*(5), 477–481. https://doi.org/10.1038/nclimate1725

Saxton, K. E., Rawls, W., Romberger, J. S., & Papendick, R. I. (1986). Estimating generalized soil-water characteristics from texture. *Soil Science Society of America Journal*, *50*(4), 1031–1036. https://doi.org/10.2136/sssaj1986.03615995005000040054x

Schieder, N. W., & Kirwan, M. L. (2019). Sea-level driven acceleration in coastal forest retreat. *Geology*, *47*(12), 1151–1155. https://doi.org/10.1130/g46607.1

Shah, S. H. H., Vervoort, R. W., Suweis, S., Guswa, A. J., Rinaldo, A. S. E. A. T. M., & Van Der Zee, S. E. A. T. M. (2011). Stochastic modeling of salt accumulation in the root zone due to capillary flux from brackish groundwater. *Water Resources Research*, *47*(9). https://doi.org/10.1029/2010wr009790

Shokri, N., Zhou, P., & Keshmiri, A. (2015). Patterns of desiccation cracks in saline bentonite layers. *Transport in Porous Media*, *110*(2), 333–344. https://doi.org/10.1007/s11242-015-0521-x

Simmons, C., Bauer-Gottwein, P., Graf, T., Kinzelbach, W., Kooi, H., Li, L., et al. (2010). *Variable density groundwater flow: From modelling to applications*. Doctoral dissertation. Cambridge University Press.

Simmons, C. T. (2005). Variable density groundwater flow: From current challenges to future possibilities. *Hydrogeology Journal*, *13*(1), 116–119. https://doi.org/10.1007/s10040-004-0408-3

Šimůnek, J., Šejna, M., & Van Genuchten, M. T. (2018). New features of version 3 of the HYDRUS (2D/3D) computer software package. *Journal of Hydrology and Hydromechanics*, *66*(2), 133–142. https://doi.org/10.1515/johh-2017-0050

Smets, S. M. P., Kuper, M., Van Dam, J. C., & Feddes, R. A. (1997). Salinization and crop transpiration of irrigated fields in Pakistan's Punjab. *Agricultural Water Management*, *35*(1–2), 43–60. https://doi.org/10.1016/s0378-3774(97)00031-0

Song, J., Yang, Y., Wu, J., & Wu, J. (2022). The coastal aquifer recovery subject to storm surge: Effects of connected heterogeneity, physical barrier and surge frequency. *Journal of Hydrology*, *610*, 127835. https://doi.org/10.1016/j.jhydrol.2022.127835

Stanic, S., LeRoux, N. K., Paldor, A., Mohammed, A. A., Michael, H. A., & Kurylyk, B. L. (2024). Saltwater intrusion into a confined island aquifer driven by erosion, changing recharge, sea-level rise, and coastal flooding. *Water Resources Research*, *60*(1), e2023WR036394. https://doi.org/10.1029/2023wr036394

Sumner, D. M., & Belaineh, G. (2005). Evaporation, precipitation, and associated salinity changes at a humid, subtropical estuary. *Estuaries*, *28*(6), 844–855. https://doi.org/10.1007/bf02696014

Tahir, S., & Marschner, P. (2017). Clay addition to sandy soil reduces nutrient leaching—Effect of clay concentration and ped size. *Communications in Soil Science and Plant Analysis*, *48*(15), 1813–1821. https://doi.org/10.1080/00103624.2017.1395454

Tan, X., Shao, D., Gu, W., & Liu, H. (2015). Field analysis of water and nitrogen fate in lowland paddy fields under different water managements using HYDRUS-1D. *Agricultural Water Management*, *150*, 67–80. https://doi.org/10.1016/j.agwat.2014.12.005

Terry, J. P., & Falkland, A. C. (2010). Responses of atoll freshwater lenses to storm-surge overwash in the Northern Cook Islands. *Hydrogeology Journal*, *18*(3), 749–759. https://doi.org/10.1007/s10040-009-0544-x

Uchida, R. (2000). Essential nutrients for plant growth: Nutrient functions and deficiency symptoms. *Plant Nutrient Management in Hawaii's Soils*, *4*, 31–55.

Valentine, K., Herbert, E. R., Walters, D. C., Chen, Y., Smith, A. J., & Kirwan, M. L. (2023). Climate-driven tradeoffs between landscape connectivity and the maintenance of the coastal carbon sink. *Nature Communications*, *14*(1), 1137. https://doi.org/10.1038/s41467-023-36803-7

Van Biersel, T. P., Carlson, D. A., & Milner, L. R. (2007). Impact of hurricanes storm surges on the groundwater resources. *Environmental Geology*, *53*(4), 813–826. https://doi.org/10.1007/s00254-007-0694-x

Vanderborght, J., & Vereecken, H. (2007). Review of dispersivities for transport modeling in soils. *Vadose Zone Journal*, *6*(1), 29–52. https://doi.org/10.2136/vzj2006.0096

Van Genuchten, M. T. (1980). A closed-form equation for predicting the hydraulic conductivity of unsaturated soils. *Soil Science Society of America Journal*, *44*(5), 892–898. https://doi.org/10.2136/sssaj1980.03615995004400050002x

Wang, T., Xu, Y., Zuo, Q., Shi, J., Wu, X., Liu, L., et al. (2023). Evaluating and improving soil water and salinity stress response functions for root water uptake. *Agricultural Water Management*, *287*, 108451. https://doi.org/10.1016/j.agwat.2023.108451

Wang, W., Zhang, P., Zhang, H., Grossiord, C., Pennington, S. C., Norwood, M. J., et al. (2022). Severe declines in hydraulic capacity and associated carbon starvation drive mortality in seawater exposed Sitka-spruce (Picea sitchensis) trees. *Environmental Research Communications*, *4*(3), 035005. https://doi.org/10.1088/2515-7620/ac5f7d

Warnell, K., Olander, L., & Currin, C. (2022). Sea level rise drives carbon and habitat loss in the US mid-Atlantic coastal zone. *PLoS Climate*, *1*(6), e0000044. https://doi.org/10.1371/journal.pclm.0000044

Werner, A. D., Bakker, M., Post, V. E., Vandenbohede, A., Lu, C., Ataie-Ashtiani, B., et al. (2013). Seawater intrusion processes, investigation and management: Recent advances and future challenges. *Advances in Water Resources*, *51*, 3–26. https://doi.org/10.1016/j.advwatres.2012.03.004

Williams, K., Ewel, K. C., Stumpf, R. P., Putz, F. E., & Workman, T. W. (1999). Sea-level rise and coastal forest retreat on the west coast of Florida, USA. *Ecology*, *80*(6), 2045–2063. https://doi.org/10.2307/176677

Woods, N. N., Swall, J. L., & Zinnert, J. C. (2020). Soil salinity impacts future community composition of coastal forests. *Wetlands*, *40*(5), 1495–1503. https://doi.org/10.1007/s13157-020-01304-6

Xiao, H., Wang, D., Medeiros, S. C., Bilskie, M. V., Hagen, S. C., & Hall, C. R. (2019). Exploration of the effects of storm surge on the extent of saltwater intrusion into the surficial aquifer in coastal east-central Florida (USA). *The Science of the Total Environment*, *648*, 1002–1017. https://doi.org/10.1016/j.scitotenv.2018.08.199

Xu, X., Zhang, Q., Li, Y., & Li, X. (2016). Evaluating the influence of water table depth on transpiration of two vegetation communities in a lake floodplain wetland. *Hydrology Research*, *47*(S1), 293–312. https://doi.org/10.2166/nh.2016.011

Yang, J., Zhang, H., Yu, X., Graf, T., & Michael, H. A. (2018). Impact of hydrogeological factors on groundwater salinization due to ocean-surge inundation. *Advances in Water Resources*, *111*, 423–434. https://doi.org/10.1016/j.advwatres.2017.11.017

Yang, T., Šimůnek, J., Mo, M., Mccullough-Sanden, B., Shahrokhnia, H., Cherchian, S., & Wu, L. (2019). Assessing salinity leaching efficiency in three soils by the HYDRUS-1D and-2D simulations. *Soil and Tillage Research*, *194*, 104342. https://doi.org/10.1016/j.still.2019.104342

Younes, A., Koohbor, B., Belfort, B., Ackerer, P., Doummar, J., & Fahs, M. (2022). Modeling variable-density flow in saturated-unsaturated porous media: An advanced numerical model. *Advances in Water Resources*, *159*, 104077. https://doi.org/10.1016/j.advwatres.2021.104077

Yu, C., Cheng, J. J., Jones, L. G., Wang, Y. Y., Faillace, E., Loureiro, C., & Chia, Y. P. (1993). *Data collection handbook to support modeling the impacts of radioactive material in soil (No. ANL/EAIS--8)*. Argonne National Lab.

Yu, X., Xin, P., & Hong, L. (2021). Effect of evaporation on soil salinization caused by ocean surge inundation. *Journal of Hydrology*, *597*, 126200. https://doi.org/10.1016/j.jhydrol.2021.126200

Yu, X., Yang, J., Graf, T., Koneshloo, M., O'Neal, M. A., & Michael, H. A. (2016). Impact of topography on groundwater salinization due to ocean surge inundation. *Water Resources Research*, *52*(8), 5794–5812. https://doi.org/10.1002/2016wr018814

Zeng, W., Xu, C., Wu, J., & Huang, J. (2014). Soil salt leaching under different irrigation regimes: HYDRUS-1D modelling and analysis. *Journal of Arid Land*, *6*(1), 44–58. https://doi.org/10.1007/s40333-013-0176-9

Zhang, X. D., Chen, Y. G., Ye, W. M., Cui, Y. J., Deng, Y. F., & Chen, B. (2017). Effect of salt concentration on desiccation cracking behavior of GMZ bentonite. *Environmental Earth Sciences*, *76*(15), 1–10. https://doi.org/10.1007/s12665-017-6872-6